Effect of Ridge Width on the Lasing Characteristics of Triangular and Rectangular InAs/In<inf>0.53</inf>Ga<inf>0.47</inf>As Quantum Well

frontiers in Materials

ORIGINAL RESEARCH
published: 26 January 2022
doi: 10.3389/fmats.2022.833777

Effect of Ridge Width on the Lasing Characteristics of Triangular and Rectangular InAs/$In_{0.53}Ga_{0.47}As$ Quantum Well Lasers

Zhejing Jiao[1], *Yi Gu*[2,3]*, *Yonggang Zhang*[2,3], *Anduo Hu*[1], *Qian Gong*[3], *Shumin Wang*[4], *Tao Li*[2] *and Xue Li*[2]

[1]College of Electronics and Information Engineering, Shanghai University of Electric Power, Shanghai, China, [2]State Key Laboratory of Transducer Technology, Shanghai Institute of Technical Physics, Chinese Academy of Sciences, Shanghai, China, [3]Key Laboratory of Terahertz Technology, Shanghai Institute of Microsystem and Information Technology, Chinese Academy of Sciences, Shanghai, China, [4]Department of Microtechnology and Nanoscience, Chalmers University of Technology, Gothenburg, Sweden

The lasing characteristics of InP-based InAs/$In_{0.53}Ga_{0.47}As$ quantum well (QW) lasers with different ridge widths are investigated. Two groups of lasers are grown for comparison, one with active triangular QW regions and the other with rectangular QW regions. Their output powers, characteristic temperatures (T_0), external differential quantum efficiencies (η_d) and junction temperatures (T_j) are analyzed and compared. The parameter of ridge width is found to play an important role in the performance of the lasers. In triangular QW lasers, by broadening the ridge width from 8 to 12 μm, output power and η_d of the lasers are decreased for the temperature range of 100–320 K due to heating effect. But by broadening the ridge width from 8 to 100 μm in rectangular QW lasers, output power has about 3.5 time increase at 100 K and η_d also has a little increase for temperatures from 100 to 180 K due to much larger emission area and much faster heat dissipation. T_j, the real temperature of the active region, is also found to have accelerated increase at high injection current and heat sink temperature. Besides, compared to the rectangular QW laser of the same ridge width, the improved thermal performance of triangular QW laser is also demonstrated.

Keywords: InAs quantum wells, lasing characteristics, ridge width effect, triangular quantum wells, rectangular quantum wells

OPEN ACCESS

Edited by:
Tao Wang,
the University of Sheffield,
United Kingdom

Reviewed by:
Guoen Weng,
East China Normal University, China
Tao Wang,
Hangzhou Dianzi University, China

***Correspondence:**
Yi Gu
guyi@mail.sitp.ac.cn

Specialty section:
This article was submitted to Semiconducting Materials and Devices, a section of the journal Frontiers in Materials

Received: *12 December 2021*
Accepted: *10 January 2022*
Published: *26 January 2022*

Citation:
Jiao Z, Gu Y, Zhang Y, Hu A, Gong Q, Wang S, Li T and Li X (2022) Effect of Ridge Width on the Lasing Characteristics of Triangular and Rectangular InAs/$In_{0.53}Ga_{0.47}As$ Quantum Well Lasers. Front. Mater. 9:833777. doi: 10.3389/fmats.2022.833777

INTRODUCTION

Semiconductor lasers are desirable for applications of molecular spectroscopy, gas sensing (Tittel et al., 2003; Zhang et al. 2021a; Zhang et al. 2021b) and medical diagnostics (Jean and Bende 2003), etc. For the wavelength range of around 2 μm, GaSb-based semiconductor materials are traditionally developed (Zhang et al., 2006; Jiang et al., 2021; Calvo et al., 2020). Besides, $In_xGa_{1-x}As/In_{0.53}Ga_{0.47}As$ (x > 0.53) quantum well (QW) structure on InP substrate is an alternative method for this wavelength range, which has the advantages of relatively mature growth and processing technology (Serries et al., 2001; Sato et al., 2005). In this structure, the well width and numbers of QWs can be adjusted to extend the emission wavelength and improve the laser performance. T. Sato found that the temperature characteristics of the laser with 5 nm thick InAs wells is better than

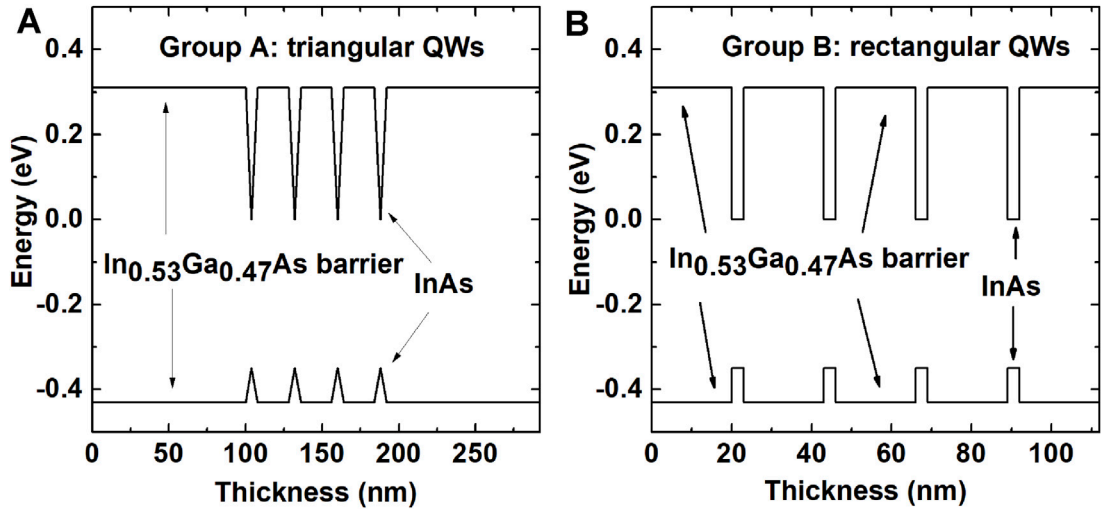

FIGURE 1 | Schematic energy-band diagrams of **(A)** group A lasers with triangular QWs and **(B)** group B lasers with rectangular QWs as active regions.

those of the laser with 3 nm thick InAs wells (Sato et al., 2008). Y. Gu et al. designed a group of AlInGaAs/InGaAs/InAs samples with different well widths of 9–25 nm, and found that the material quality can be improved by adjusting the well width (Gu et al., 2009). The well shapes, rectangular or triangular, also play an important role in the output characteristics of the lasers. In ref (Cao et al., 2014), the threshold current density, output power and characteristic temperature were improved remarkably by adopting triangular QWs in the active region of InAs/InGaAs QW lasers.

Besides, ridge width is another important factor that might affect the laser performance. There are reports on the ridge width dependence in $In_{0.64}Ga_{0.36}As/In_{0.38}Al_{0.62}As$ quantum cascade lasers at 6 μm (Slivken et al., 2004), InAs/InP quantum-dash lasers at 1.6 μm (Alkhazraji et al., 2018), and InGaAsP/InP QW lasers at 1.3 μm (Huang et al., 1997). Improved lasing characteristics are obtained in these lasers as ridge width narrows. However, there is no study on the ridge width effect on the performance of InAs/InP QW lasers emitting in the mid-infrared range.

In this work, the effect of ridge width on the lasing characteristics of InAs/InP QW lasers emission at about 2 μm is investigated. The continuous wave (CW) output power, threshold current densities (J_{th}), characteristic temperatures (T_0), external differential quantum efficiencies (η_d) and junction temperatures (T_j) for the triangular QWs with ridge widths of 8, 10, and 12 μm and for the rectangular QWs with ridge widths of 8 and 100 μm are compared and analyzed. The 8-μm ridge laser has the highest output power under the same injection current and η_d among the three triangular QW lasers due to lower local heating effect with a narrower ridge width. But in the rectangular QW lasers, although the maximum operation temperature is lower in the 100-μm ridge laser, it has a higher output power and η_d at low temperatures due to better heat dissipation in an enlarged active region area, which can compensate the heating effect by a high injection current to some extent. The T_j-values as a function of injection current at different heat sink temperatures are also calculated and compared. In addition, by comparing the two 8-μm ridge lasers, it is found that the triangular QW laser has better lasing and thermal performance than those of the rectangular QW lasers.

DEVICE FABRICATION

Two groups of samples were epitaxially grown on n-type (001)-oriented InP epi-ready substrates in a VG Semicon V80H gas source molecular beam epitaxy (GSMBE) system. In both groups, the growth started from a 1,000-nm n-type InP buffer layer, followed by a 120-nm undoped InGaAsP waveguide layer. Then the active QW regions consisting of four QW layers, sandwiched between 20-nm $In_{0.53}Ga_{0.47}As$ barrier layers, were grown. The first and the last barrier layers are 100-nm thick in group A and 20-nm thick in group B as shown in the schematic energy band diagrams in **Figure 1**. Also, as shown in **Figure 1**, the QW layers in groups A and B are 8-nm-thick $InAs/In_{0.53}Ga_{0.47}As$ triangular layers and 3-nm-thick rectangular InAs layers, respectively. The details of the growth of triangular QW layers using digital alloy technology can be found in ref (Gu et al., 2014). The triangular QWs were equivalently formed by $InAs/In_{0.53}Ga_{0.47}As$ digital alloy with a very thin period thickness of 1 nm, without any growth interruption during the QW growth. Afterwards, a 120-nm InGaAsP upper waveguide, a 1700-nm p-type doped InP upper cladding layer and a 300-nm $In_{0.53}Ga_{0.47}As$ contact layer were grown. The growth temperatures were kept the same for groups A and B samples.

The epitaxial growths for both groups of pseudomorphic QW structures have been well-studied without observed dislocations. The transmission electron microscope (TEM) images of triangular QWs with similar material and structures have been reported where clear interface between layers without visible threading or misfit dislocations are observed, indicating good crystal quality (Gu et al., 2010). For the rectangular QWs, the crystal quality is usually good for the structures with QW thickness smaller than

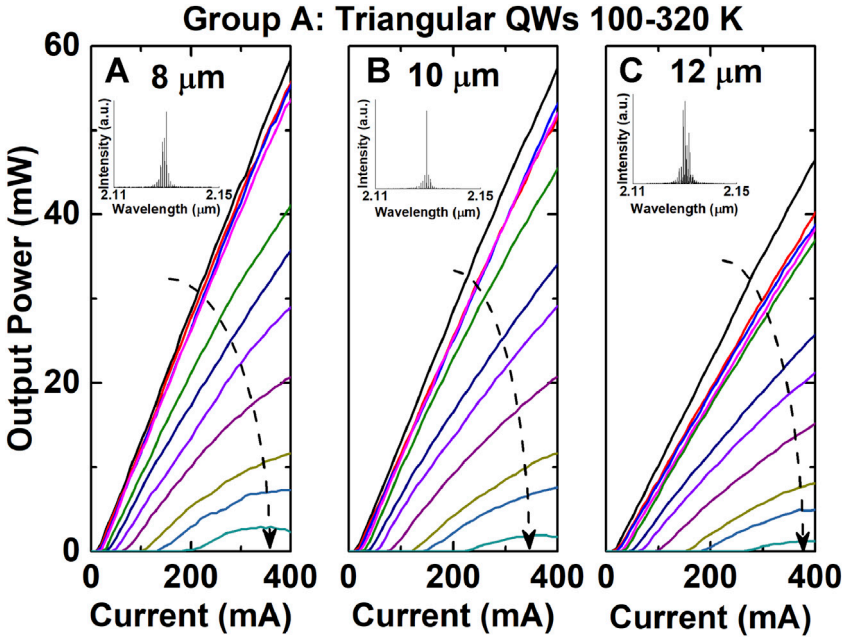

FIGURE 2 | Output power versus current with temperatures from 100 to 320 K for group A (triangular QW) lasers with ridge widths of **(A)** 8, **(B)** 10, and **(C)** 12 μm, respectively. The insets show the output spectra at 300 K for the three lasers at threshold current, respectively.

5 nm. The TEM image of similar material structures can be also found in literatures with distinct interfaces (Sato et al., 2007). Therefore, it is believed both groups of samples have good material quality for further fabrication into lasers.

Next, the samples were fabricated into ridge waveguide lasers using standard lithography and wet chemical etching. The effect of ridge width with ridge size in a large range is expected to be investigated by limited samples. Therefore, different ridge width ranges are used for the two groups. The ridge widths were designed to be 8, 10, and 12 μm for lasers of group A, and 8 and 100 μm for lasers of group B. 300-nm Si_3N_4 layers were deposited by plasma enhanced chemical vapor deposition for isolation. And 4, 6, 6, and 92-μm wide windows were open on the top of the 8, 10, 12, and 100-μm ridges, respectively. Sputtered Ti/Pt/Au was formed as top p-type contact and evaporated Ge/Au/Ni/Au as back bottom n-type contact. The laser chips were then diced into bars of 800 μm with as-cleaved facets, mounted on copper heat sinks and wire bonded.

The lasers were driven by CW current using a Keithley 2420 source meter. The temperature was controlled by an Oxford Optistat DN-V variable temperature liquid nitrogen cryostat. A Coherent EMP 1000 power meter was used for the I-P measurements and the spectral characteristics were measured by a Nicolet 860 Fourier transform infrared (FTIR) spectrometer.

RESULTS AND DISCUSSIONS

Output Power P_{out}

The output power versus CW driving current at temperatures from 100 to 320 K for lasers with triangular QWs (group A) are shown in **Figure 2**. In **Figures 2A–C**, the ridge widths of the three lasers are 8, 10, and 12 μm, respectively and the cavity lengths are all 0.8 mm. The emission wavelengths are around 2.13 μm for the three lasers at 300 K as shown in the insets of **Figure 2**. And the maximum operation temperatures are all 320 K. At 400 mA, the output power per facet is about 56 mW at 100 K and 11.6 mW at 300 K for the laser with 8-μm ridge width. The output powers are 57 mW at 100 K and 11.5 mW at 300 K for the laser with 10-μm-ridge width at 400 mA. It can be seen from the figure that the 12-μm-ridge laser has the lowest output power for all temperatures. Compared to the other two lasers with narrower ridge widths, the output power per facet of the 12-μm-ridge laser at 400 mA is only about 46 mW at 100 K and 8 mW at 300 K, corresponding to a decrease by 21.7% and 31%, respectively. A higher driving current is required for the laser with a wider ridge width, resulting in a higher junction temperature as well as intensified non-radiative recombinations within the device. The opening of the top contact of the 12-μm ridge is only 6-μm, the same as that of the 10-μm ridge, might also lead to a high local temperature at a high injection current and reduce the output power. So the output power decreases with the increase of ridge width from 8 to 12 μm due to local heating effect.

For group B lasers, the shape of the active QWs is rectangular. The ridge widths of group B lasers are 8 and 100 μm, respectively, and the cavity lengths are also 0.8 mm. The output power versus CW driving current is shown in **Figure 3**. The emission wavelengths are about 2.17 μm at 290 K and 2.1 μm at 200 K for the two lasers, respectively as shown in the insets of **Figures 3A,B**. The maximum operation temperatures are 290 K for the 8-μm ridge laser and 200 K for the 100-μm ridge laser. It can be seen that the maximum operation temperature depends strongly on

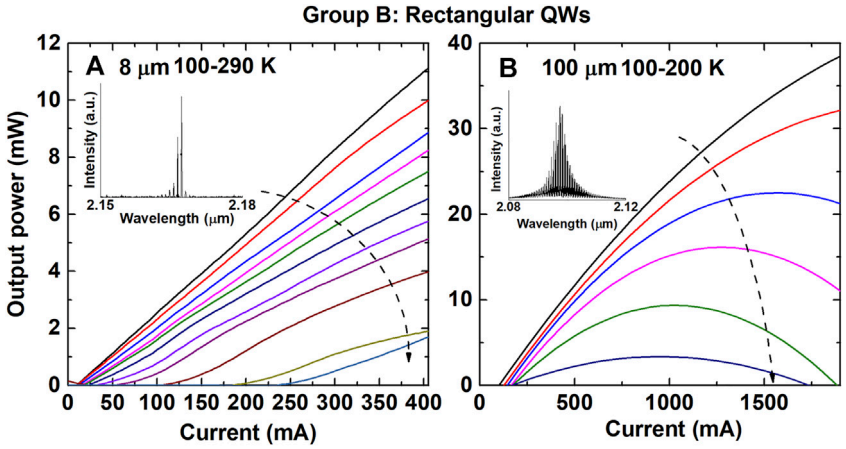

FIGURE 3 | Output power versus current for **(A)** the 8-μm ridge laser from 100 to 290 K and **(B)** the 100-μm ridge laser from 100 to 200 K for group B (rectangular QW) lasers. The insets show the output spectra at 290 and 200 K at 1.2 times of the threshold current for the two lasers, respectively. Note that the current ranges are 0–400 mA in **(A)** and 0–1900 mA in **(B)**, respectively.

the ridge width due to heating effect. For the 8-μm ridge laser, the output power per facet is 11 mW at 100 K with a driving current of 405 mA. Note that the driving current for this laser is restricted to be below 405 mA to avoid the damage of the laser. For the 100-μm ridge laser, the output power is 38 mW at 1.9 A at 100 K, about 3.5 times that of the 8-μm ridge laser. Although there is a stronger heating effect within the 100-μm ridge laser, it has a much broader emission area and thus higher output power. However, the increase of output power is not proportional to the increase of ridge width. And with temperature further increased, the output power rolls over with the driving current for the 100-μm ridge laser due to the local heating effect.

The 8-μm ridge laser in group B has a lower maximum operation temperature than that of the laser with the same ridge width in group A. For the temperatures of 100–300 K, the output power of the 8-μm ridge laser in group B has a decrease of more than 80% compared with that of the 8-μm ridge laser in group A. Note that the average lattice mismatch is about 1.71×10^{-2} for the triangular InAs/$In_{0.53}Ga_{0.47}As$ QW, while it is 3.38×10^{-2} for the rectangular InAs/$In_{0.53}Ga_{0.47}As$ QW. So the accumulated strain defined as the average lattice mismatch times the QW thickness is larger for the 8 nm triangular QWs than that with the 3 nm rectangular QWs. However, the triangular QW lasers have shown much higher output power with larger strains, indicating improved performance with triangular active regions.

The two 8-μm ridge lasers have different materials in the active region and different thickness of the first and last barrier layers, which might affect the optical confinement factor (Γ) of the lasers. The equivalent refractive index of the triangular InAs/$In_{0.53}Ga_{0.47}As$ QWs is about 3.47 (Cao, 2014), very close to the refractive index of InAs of 3.45 (Adachi, 1989), the difference of which has limited influence on the Γ parameter. Also, by thickening both the first and last barriers from 20 to 100 nm in triangular QWs, the Γ parameter is found to increase only from 0.437 to 0.475 (Cao, 2014). That is to say, the two 8-μm ridge lasers have very close Γ values, which has almost no effect on the output power of the two lasers.

Characteristic Temperature T_0

The threshold current density J_{th} under CW driving conditions for the two groups of lasers are shown in **Figure 4**. In group A, the J_{th} values for the three ridge widths are very close in the whole temperature range. There exist three different slopes of the natural logarithm of J_{th} in the figure. The T_0-values are extracted by linear fitting of J_{th} for the three temperature ranges of 100–200 K, 200–300 K, and 300–320 K. For the 8-μm ridge laser, T_0 is derived to be about 174 K in the temperature range of 100–200 K, and decreased to 72 and 31 K in the temperature ranges of 200–300 K and 300–320 K, respectively. For both 10-μm and 12-μm-ridge lasers, the T_0 is 119 K at the temperature range of 100–200 K, smaller than that of the 8-μm ridge laser. The T_0-values of lasers in group A are very close at the two higher temperature ranges. On the whole, the three lasers have similar temperature sensitivity at high temperatures where no big change in T_0 is found with ridge widths from 8 to 12 μm.

By linearly fitting the J_{th} data for the 8-μm ridge laser in group B, the T_0-values are derived to be 112 and 37 K for the two temperature ranges of 100–180 K and 200–290 K, respectively. By the same fitting, the T_0 is 114 K for the 100-μm ridge laser with temperatures from 100–140 K, indicating similar temperature sensitivity as the narrower 8-μm ridge laser for this low temperature range. From 160 to 200 K, the J_{th}-values of the 100-μm ridge laser might have large deviation from the actual values due to the rolling off effect, and thus they are not included in the fitting.

In both groups, J_{th} slightly increases as the ridge width narrows as reported in (Liu et al., 2006). By comparing the two 8-μm ridge lasers in the two groups, it is seen that the laser with the triangular QWs has higher T_0-values and thus is less

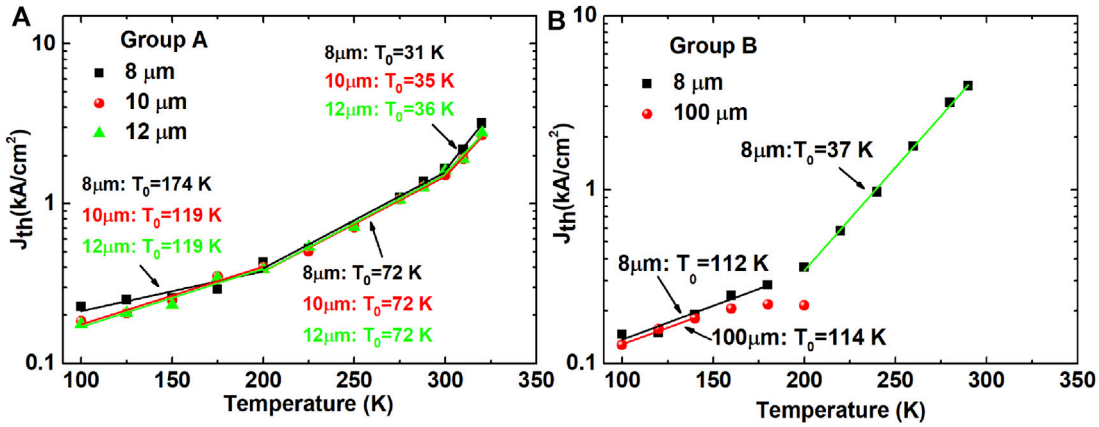

FIGURE 4 | Temperature dependent threshold current density J_{th} for lasers in **(A)** group A and **(B)** group B. The symbols are experimental data. The solid lines are fitting lines of ln (J_{th}) in different temperature ranges. Group A: 100–200 K, 200–300 K, and 300–320 K; Group B: 100–180 K and 200–290 K for the 8-μm ridge laser, and 100–140 K for the 100-μm ridge laser.

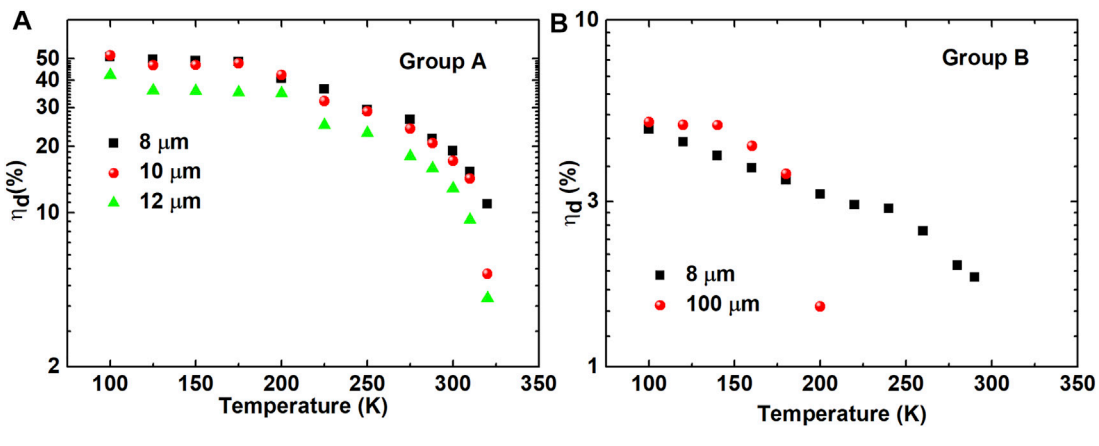

FIGURE 5 | External differential quantum efficiencies η_d at different temperatures for **(A)** group A and **(B)** group B lasers.

sensitive to temperature than the laser with the rectangular QWs.

External Differential Quantum Efficiency η_d

The external differential quantum efficiency as a function of the operation temperature for the lasers of the two groups is shown in **Figure 5**. The η_d is 51% at 100 K and drops to 11% at 320 K for the 8-μm ridge laser in group A. The 10-μm ridge laser has similar η_d values at the low temperature range of 100–200 K, but it drops faster as temperature increases, which is only 5% at 320 K. It can be observed from the figure that the η_d of the 12-μm ridge laser is only 42% at 100 K and 4% at 320 K, which is the lowest among the three group A lasers for the whole temperature range. The efficiency has a decrease of about 17.6% at 100 K and 63.6% at 320 K with ridge widths increase from 8 to 12 μm due to the heating effect.

The η_d-values are very low for lasers in group B, which is only 4.8% for the 8-μm ridge laser and 5.1% for the 100-μm ridge laser at 100 K. The η_d-values are slightly higher with the 100-μm ridge laser for the temperature range of 100–180 K, but it drops very fast at the maximum operation temperature of 200 K. Although a high injection current could lead to a high local temperature, the η_d is not reduced in the 100-μm ridge below 200 K, because the generated heat can dissipate more rapidly over a larger emission area. It can also be explained from the view of thermal resistance. The thermal resistance R_{th} based on a two-dimensional flow model is given by (Martin et al., 1992; Alkhazraji et al., 2018)

$$R_{th} = \frac{1}{\pi k L} ln\left(\frac{16t}{\pi w}\right) \quad (1)$$

where k is the thermal conductivity of the substrate, L is the cavity length, t is the thickness of the substrate, and w is the ridge width. The R_{th}-value is proportional to the logarithm of the width and smaller for a wider ridge. By taking k as 0.75 W/K cm for an n-InP substrate (Alkhazraji et al., 2018), L = 0.8 mm, and t = 350 μm, the R_{th}-values are calculated to be 28.68 K/W for w = 8 μm and

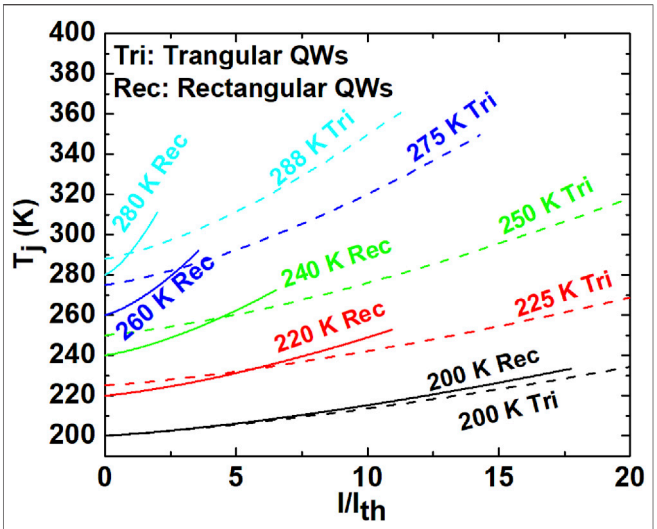

FIGURE 6 | The junction temperature T_j versus injection current for the two 8-μm ridge lasers in the two groups at different heat sink temperatures T_s from 200 to 300 K. The dash and solid lines represent T_j of the triangular and the rectangular QWs, respectively.

15.28 K/W for w = 100 μm. The laser with a wider ridge has a smaller R_{th}, which can compensate, to some extent, the temperature rise caused by a high injection current. Thus η_d does not drop easily at high temperatures.

It is also seen that the η_d is more than 10 times higher for the 8-μm ridge laser in group A compared with the laser with the same ridge width in group B in the whole temperature range of 100–290 K. This further confirms that the triangular QW lasers have better lasing characteristics than the rectangular QW lasers.

Junction Temperature T_j

The junction temperature T_j is the real temperature of the active QW regions, on which the thermal behavior of the laser critically depends. The T_j of the two 8-μm ridge lasers in the two groups are analyzed and compared. The above calculated R_{th} value is used to estimate T_j, which is given by the equation (Li et al., 2015; Alkhazraji et al., 2018),

$$T_j = T_s + R_{th}(IV - P_{out}) \quad (2)$$

where T_s is the heat sink temperature, R_{th} is the thermal resistance, I is the injection current, V is the applied voltage and P_{out} is the output power of the laser. The calculated T_j-values for the two lasers with temperatures between 200 and 300 K are plotted in **Figure 6**. For each curve (fixed T_s) in the figure, the T_j-value has a nonlinear increase with I/I_{th} especially at high I/I_{th}-values. It indicates that the difference between IV and P_{out} increases with I, dissipated in the form of non-radiative recombination. For each I/I_{th} value (fixed I/I_{th}), the T_j curve has an accelerated increase as T_s increase. For example, for the triangular QW, I/I_{th} changing from 0 to 5, the T_j has 6 K increase at T_s = 200 K but 23 K increase at T_s = 288 K. The same tendency is observed for the T_j curves of rectangular QW. This suggests that at high T_s-values, non-radiative recombination is accelerated, resulting in fast increase of junction temperature T_j.

Furthermore, it can be also seen from the figure that the T_j-values increase faster in the rectangular QW laser compared with the triangular QW laser at the same or two close temperatures, indicating more non-radiative recombination centers in the rectangular QW laser. It is seen in **Figure 5** that the rectangular QW laser has a much lower η_d-value and the majority of the injected current is converted into heat instead of light. Thus more heat is accumulated in its active region and the junction temperature is easily built up. In addition, the smaller T_j value in the triangular QW laser maybe also related to the improvement in the structure of the active region by using digital alloy technology. The increase of heat transfer across very thin layers of superlattice is predicted by some models (Chen, 1997; Simkin and Mahan, 2000). The thermal conductivity of $(AlAs)_1/(AlSb)_{11}$ digital-alloy superlattice with period of 3.6 nm is also found to be much larger than predicted by a model for thermal transport in superlattices, the possible reason of which is phonon tunneling through the thin superlattice layers (Borca-Tasciuc et al., 2009). In the active layers of our triangular QW layers, the thickness of one period including one InAs layer and one $In_{0.53}Ga_{0.47}As$ layer is only 1 nm, where phonon tunneling might also assist in the heat dissipation.

CONCLUSION

The ridge width dependence of the lasing characteristics of InAs/InP QW lasers are investigated by experiments, where a clear influence is observed. The output power and η_d have 31% and 63.6% decrease respectively at room temperature by broadening the ridge width from 8 to 12 μm in group A due to heating effect. The output power is 3.5 times in the 100-μm ridge laser compared to that of the 8-μm ridge laser in group B at 100 K and the η_d is also a little bit higher for temperatures from 100 to 180 K. It is because lasers with wide ridges have large emission area and fast heat dissipation, which can compensate the temperature rise caused by high injection current at low operation temperatures. Besides, the junction temperature values of the two groups of lasers are also found to deviate from the heat sink temperature, especially at high injection currents and operation temperatures. Furthermore, by comparing the two 8-μm ridge lasers in the two groups, it is seen that the triangular QW laser in group A has better thermal and lasing characteristics than those of the rectangular QW laser in group B in all these measured parameters. In the triangular QWs, the indium composition is graded and lower near the barrier layer, which is favorable for keeping the material quality. Besides, the critical thickness of the strain

material in the triangular QWs is also increased, indicating good material quality by using digital alloy technology. Therefore, by adopting triangular QWs in the active region, the performance of the InAs/$In_{0.53}Ga_{0.47}As$ laser on a InP substrate is improved.

DATA AVAILABILITY STATEMENT

The raw data supporting the conclusion of this article will be made available by the authors, without undue reservation.

AUTHOR CONTRIBUTIONS

ZJ: Investigation, data curation, formal analysis and writing the original draft. YG: Methodology, writing-review and editing, supervision and funding acquisition. YZ: Conceptualization and supervision. AH: Validation. QG: Supervision. SW: Writing-review, editing and funding acquisition. TL: Supervision. XL: Project administration.

FUNDING

This work was supported by the National Natural Science Foundation of China (Nos. 61704103, 61775228, 62075229, 62175250, 62104238), the Shanghai Municipal Commission of Science and Technology (No. 16ZR1412900), the International Science and Technology Cooperation Program of Shanghai (No. 20520711200), the Shanghai Rising-Star Program (No. 21QA1410600) and the Program of Shanghai Academic/Technology Research Leader (No. 21XD1404200).

REFERENCES

Adachi, S. (1989). Optical Dispersion Relations for GaP, GaAs, GaSb, InP, InAs, InSb, AlxGa1−xAs, and In1−xGaxAsyP1−y. *J. Appl. Phys.* 66, 6030–6040. doi:10.1063/1.343580

Alkhazraji, E., Khan, M. T. A., Ragheb, A. M., Fathallah, H., Qureshi, K. K., Alshebeili, S., et al. (2018). Effect of Temperature and Ridge-Width on the Lasing Characteristics of InAs/InP Quantum-Dash Lasers: A Thermal Analysis View. *Opt. Laser Tech.* 98, 67–74. doi:10.1016/j.optlastec.2017.07.039

Borca-Tasciuc, T., Song, D. W., Meyer, J. R., Vurgaftman, I., Yang, M.-J., Nosho, B. Z., et al. (2002). Thermal Conductivity of AlAs0.07Sb0.93 and Al0.9Ga0.1As0.07Sb0.93 Alloys and (AlAs)1/(AlSb)11 Digital-alloy Superlattices. *J. Appl. Phys.* 92, 4994–4998. doi:10.1063/1.1506194

Calvo, M. R., Bartolomé, L. M., Bahriz, M., Boissier, G., Cerutti, L., Rodriguez, J.-B., et al. (2020). Mid-Infrared Laser Diodes Epitaxially Grown on on-Axis (001) Silicon. *Optica* 7 (4), 263–266. doi:10.1364/OPTICA.388383

Cao, Y.-Y., Zhang, Y.-G., Gu, Y., Chen, X.-Y., Zhou, L., and Li, H.-S. -B. -Y. (2014). Improved Performance of 2.2-μm InAs/InGaAs QW Laserson InP by Using Triangular Wells. *IEEE Photon. Technol. Lett.* 26 (6), 571–574. doi:10.1109/LPT.2014.2298248

Cao, Y. Y. (2014). Study on InP-Based 2-3 μm Band Antimony-free Quantum Well Lasers. Dissertation. Shanghai, China: Shanghai Institute of Microsystem and Information Technology, University of Chinese Academy.

Chen, G. (1997). Size and Interface Effects on Thermal Conductivity of Superlattices and Periodic Thin-Film Structures. *J. Heat Transfer* 119 (2), 220–229. doi:10.1115/1.2824212

Gu, Y., Zhang, Y., Cao, Y., Zhou, L., Chen, X., Li, H., et al. (2014). 2.4 μm InP-Based Antimony-free Triangular Quantum Well Lasers in Continuous-Wave Operation above Room Temperature. *Appl. Phys. Express* 7, 032701. doi:10.7567/APEX.7.032701

Gu, Y., Zhang, Y. G., Wang, K., Li, A. Z., and Li, Y. Y. (2009). Optimization of AlInGaAs/InGaAs/InAs Strain Compensated Triangular Quantum wells Grown by Gas Source Molecular Beam Epitaxy for Laser Applications in 2.1-2.4μm Range. *J. Cryst. Growth* 311 (7), 1935–1938. doi:10.1016/j.jcrysgro.2008.10.037

Gu, Y., Wang, K., Li, Y. Y., Li, C., and Zhang, Y. G. (2010). InP-based InGaAs/InAlGaAs Digital alloy Quantum Well Laser Structure at 2 μm. *Chin. Phys. B* 19 (7), 077304. doi:10.1088/1674-1056/19/7/077304

Huang, R., Simmons, J. G., Jessop, P. E., and Evans, J. (1997). Thermal Behavior of Tensile-Strain InGaAsP-InP Lasers with Varying Ridgewidth. *IEEE Photon. Technol. Lett.* 9 (7), 889–891. doi:10.1109/68.593335

Jean, B., and Bende, T. (2003). "Mid-IR Laser Applications in Medicine," in *Topics in Applied Physics*. Editors I.T. Sorokina and K.L. Vodopyanov (Heidelberg, Berlin: Springer-Verlag), 530–565. doi:10.1007/3-540-36491-9_12

Jiang, J., Shterengas, L., Kipshidze, G., Stein, A., Belyanin, A., and Belenky, G. (2021). High-power Narrow Spectrum GaSb-Based DBR Lasers Emitting Near 21 μm. *Opt. Lett.* 46 (8), 1967–1970. doi:10.1364/OL.422536

Li, S. G., Gong, Q., Cao, C. F., Wang, X. Z., Yan, J. Y., and Wang, Y. (2015). Thermal Coefficient of InP-Based Quantum Dot Laser from Cavity-Mode Measurements. *Infrared Phys. Tech.* 68, 119–123. doi:10.1016/j.infrared.2014.11.003

Liu, C. Y., Yoon, S. F., Fan, W. J., Uddin, A., and Yuan, S. (2006). Ridge-Width Dependence on High-Temperature Continuous-Wave Operation of Native Oxide-Confined InGaAsN Triple-Quantum-Well Lasers. *IEEE Photon. Technol. Lett.* 18 (6), 791–793. doi:10.1109/LPT.2006.871697

Martin, O. J. F., Bona, G.-L., and Wolf, P. (1992). Thermal Behavior of Visible AlGaInP-GaInP Ridge Laser Diodes. *IEEE J. Quan. Electron.* 28 (11), 2582–2588. doi:10.1109/3.161317

Sato, T., Mitsuhara, M., Kakitsuka, T., Fujisawa, T., and Kondo, Y. (2008). Metalorganic Vapor Phase Epitaxial Growth of InAs/InGaAs Multiple Quantum Well Structures on InP Substrates. *IEEE J. Select. Top. Quan. Electron.* 14 (4), 992–997. doi:10.1109/JSTQE.2008.918106

Sato, T., Mitsuhara, M., and Kondo, Y. (2007). 2.33 [micro Sign]m-Wavelength InAs/InGaAs Multiple-Quantum-Well Lasers Grown by MOVPE. *Electron. Lett.* 43 (21), 1143–1145. doi:10.1049/el:20072257

Sato, T., Mitsuhara, M., Watanabe, T., and Kondo, Y. (2005). Surfactant-mediated Growth of InGaAs Multiple-Quantum-Well Lasers Emitting at 2.1μm by Metalorganic Vapor Phase Epitaxy. *Appl. Phys. Lett.* 87, 211903. doi:10.1063/1.2133920

Serries, D., Peter, M., Kiefer, R., Winkler, K., and Wagner, J. (2001). Improved Performance of 2-μm GaInAs Strained Quantum-Well Lasers on InP by Increasing Carrier Confinement. *IEEE Photon. Technol. Lett.* 13 (5), 412–414. doi:10.1109/68.920734

Simkin, M. V., and Mahan, G. D. (2000). Minimum Thermal Conductivity of Superlattices. *Phys. Rev. Lett.* 84, 927–930. doi:10.1103/PhysRevLett.84.927

Slivken, S., Yu, J. S., Evans, A., David, J., Doris, L., and Razeghi, M. (2004). Ridge-Width Dependence on High-Temperature Continuous-Wave Quantum-Cascade Laser Operation. *IEEE Photon. Technol. Lett.* 16 (3), 744–746. doi:10.1109/LPT.2004.823746

Tittel, F. K., Richter, D., and Fried, A. (2003). "Mid-Infrared Laser Applications in Spectroscopy," in *Topics in Applied Physics*. Editors I.T. Sorokina and K.L. Vodopyanov (Heidelberg, Berlin: Springer-Verlag), 458–529. doi:10.1007/3-540-36491-9_11

Zhang, H., Sun, J., Yang, J., De Leon, I., Zaccaria, R. P., Qian, H., et al. (2021b). Biosensing Performance of a Plasmonic-Grating-Based Nanolaser (Invited Paper). *Pier* 171, 159–169. doi:10.2528/PIER21092405

Zhang, H., Wang, T., Tian, J., Sun, J., Li, S., De Leon, I., et al. (2021a). Quasi-BIC Laser Enabled by High-Contrast Grating Resonator for Gas Detection. *Nanophotonics*. doi:10.1515/nanoph-2021-0368

Zhang, Y. G., Zheng, Y. L., Lin, C., Li, A. Z., and Liu, S. (2006). Continuous Wave Performance and Tunability of MBE Grown 2.1μm InGaAsSb/AlGaAsSb MQW Lasers. *Chin. Phys. Lett.* 23 (8), 2262–2265.

Conflict of Interest: The authors declare that the research was conducted in the absence of any commercial or financial relationships that could be construed as a potential conflict of interest.

Publisher's Note: All claims expressed in this article are solely those of the authors and do not necessarily represent those of their affiliated organizations, or those of the publisher, the editors and the reviewers. Any product that may be evaluated in this article, or claim that may be made by its manufacturer, is not guaranteed or endorsed by the publisher.